

# *0.18 $\mu\text{m}$ CMOS power amplifier architecture comparison for a wideband Doherty configuration*

*Aleksandr Vasjanov, Vaidotas Barzdenas*

*Department of Computer Engineering, Vilnius Gediminas Technical University, Vilnius, Lithuania*

**Abstract:** This paper presents a comparison between a classical and a self-biased two stage CMOS power amplifier (PA) suitable for a wideband Doherty (DPA) configuration. Both PAs are fully differential and have been implemented in IBM 7RF 0.18  $\mu\text{m}$  CMOS process and are supplied from 1.8 V. Classical PA input impedance is shown to be matched from 1.6 GHz to 2.7 GHz @  $S_{11} = -10$  dB with external matching components. Self-biased PA is matched from 800 MHz to 1.75 GHz without any additional matching components and the bandwidth can be further increased to 2.15 GHz. Self-biased PA average PAE is 25.3 % which is 4.2 % higher than that of the classic PA. Both power amplifiers have an average output power of 10.5 dBm. The latter results show, that a self-biased PA architecture has more potential to be implemented in a wideband DPA configuration, compared to the classic PA arrangement. The active area for both on-chip PAs is 800  $\mu\text{m}^2$ , whereas the full IC chip size is 1.5  $\text{mm}^2$ . The dual PA ASIC has been designed to be enclosed in a 20-pin QFN package.

**Keywords:** CMOS; Power amplifier; Self-biased; Doherty; Wideband

## *Primerjava 0.18 $\mu\text{m}$ CMOS arhitektur močnostnih ojačevalnikov za širokopasovno Doherty konfiguracijo*

**Izvleček:** Članek predstavlja primerjavo med klasičnim in samonastavljivim dvostopenjskim CMOS močnostnim ojačevalnikom (PA) za širokopasovno Doherty (DPA) konfiguracijo. Oba sta popolnoma diferencialna in izvedena v 0.18  $\mu\text{m}$  IBM 7RF CMOS tehnologiji. Napajana sta z 1.8 V. Vhodna impedanca klasičnega ojačevalnika se ujema od 1.6 GHz do 2.7 GHz @  $S_{11} = -10$  dB z zunanjimi ujemalnimi komponentami. Samonastavljivi ojačevalnik je ustrezen od 800 MHz do 1.7 GHz brez dodatnih zunanjih komponent. Njegovna pasovna širina se lahko razširi do 2.15 GHz. Povprečen PAE je 25.3%, kar je 4.2% več kot pri klasičnem ojačevalniku. Oba ojačevalnika imata izhodno moč 10 dBm, kar nakazuje, da je samonastavljivi ojačevalnik bolj primeren za širokopasovne DPA konfiguracije. Površina obeh je 800  $\mu\text{m}^2$ , pri velikosti čipa 1.5  $\text{mm}^2$ . Dvojni PA ASIC je bil dimenzioniran, da ustreza 20-pinski QFN ohišju.

**Ključne besede:** CMOS; močnostni ojačevalnik; samonastavljiv; Doherty; široki pas

\* Corresponding Author's e-mail: [aleksandr.vasjanov@vgtu.lt](mailto:aleksandr.vasjanov@vgtu.lt)

### *1 Introduction*

Over the past decade, the number of papers published on power amplifier (PA) research has been increasing exponentially. Since then different PA efficiency enhancement techniques and architectures have been proposed and the Doherty power amplifier (DPA) arrangement is one of the most promising [1]. The vast majority of published papers present single-ended or differential Doherty power amplifiers designed using a classical PA topology. Only classical, cascode PAs with either common inductors, slab inductors or baluns implemented in a DPA have been researched [3-14]. This

article presents a comparison between a classical two stage power amplifier and a self-biased PA approach both suitable to be implemented in a wideband DPA. This paper is arranged as follows: DPA design challenges and a performance comparison between the published DPAs are presented in the second chapter. The proposed classical and self-biased PA architectures are presented and thoroughly analyzed in the next chapter. Simulation results and full ASIC layout are presented in the following chapter. Finally conclusions are made and references are given.

## 2 Doherty power amplifier design challenges

Multiple power amplifier architectures have been published in research papers over the last decade, including classic, cascode, self-biased PA configurations employing different parameter improvement techniques such as feedback, feedforward or/and linearization circuits. One of the most promising advanced PA architecture – Doherty power amplifier (DPA) presented in Figure 1 – provides a combination of high linearity and sufficient PAE at input powers ranging from back-off power to P1dB. Although DPAs prove to be very efficient at a certain frequency, there are several drawbacks in the architecture which restrict performance over wide bandwidth. The first drawback is the bandwidth of the classical output impedance inverter, which enhances the DPA to utilize loadpull in order to achieve high efficiency. This has been addressed in [2] and it has been proven, that the proposed impedance inverter can be designed in such a way that has more than 83 % of fractional bandwidth. Another DPA drawback is the inevitable result nonlinear nature of the peak amplifier. The peak amplifier is typically biased in class C [15] and requires harmonic termination. A harmonic termination circuit is essentially a series LC circuit (resonator) connected as a shunt to the output of the peak amplifier. Consequently for a larger DPA bandwidth several switchable harmonic terminations may be used.

Table 1 summarizes published CMOS DPA parameters. The latter table reveals, that the scaling of CMOS process does not improve the main design criterion for the always power hungry PA – power added efficiency (PAE). According to Table 1 CMOS processes in the range from 0.18  $\mu\text{m}$  to 0.13  $\mu\text{m}$  provide the largest DPA efficiency. Moreover, the latter processes are have been around since 1999-2001, therefore the relation be-

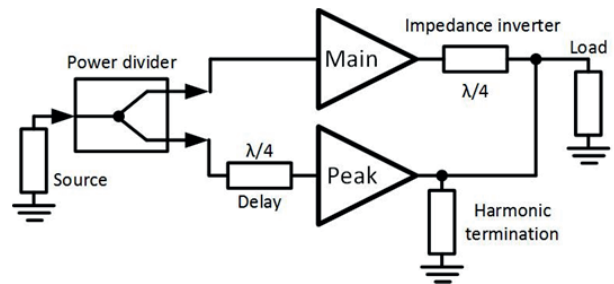


**Figure 1:** Classic Doherty power amplifier block diagram

tween the performance and price per chip area can be very attractive for DPA designers and researchers.

## 3 Power amplifier architectures for wideband Doherty configuration

The simplified single-ended classic two-stage cascode PA is presented in Figure 2. The latter PA input and output stages are biased from internal sources for AB class operation. Cascoding in both stages has been chosen in order to reduce the influence of Miller effect and improve both isolation and stability. Gain control has been implemented to toggle the cascode transistors in both stages through on-chip buffers.

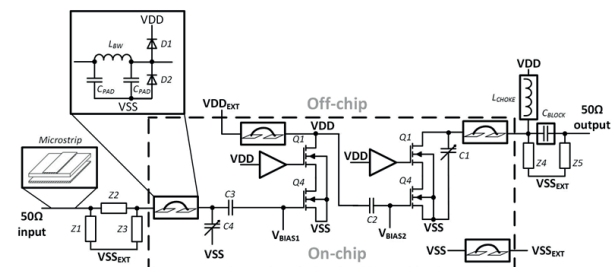


**Figure 2:** Classic two stage single ended power amplifier simplified schematic

**Table 1:** CMOS Doherty power amplifier performance comparison

Ref.	Process	VDD, V	Frequency, GHz	P1dB, dBm	Overall PAE, %	Power back-off, dB
3	0.18 $\mu\text{m}$ CMOS	3.7	3.5	24.4	36.1	6.0
4	0.18 $\mu\text{m}$ CMOS	3.3	2.4	29.5	22.0	5.0
5	0.18 $\mu\text{m}$ CMOS	3.0	2.4	22.6	31.0	7.0
6	0.18 $\mu\text{m}$ CMOS	-	0.89	25.0	43.6	5.0
7	0.13 $\mu\text{m}$ CMOS	3.3	2.4	31.9	30.1	5.0
8	0.13 $\mu\text{m}$ CMOS	3.3	1.7	31.7	33.0	5.0
9	0.13 $\mu\text{m}$ CMOS	3.0	2.4	22.0	45.0	7.0
10	90 nm CMOS	3.3	2.4	30.0	24.0	5.0
11	90 nm CMOS	2.4	2.4	24.8	26.0	5.0
12	65 nm CMOS	5.5	2.535	23.4	25.0	8.5
13	65 nm CMOS	3.3	2.4	33.5	20.0	5.0
14	65 nm CMOS	2.5	2.4	23.4	24.7	7.0

The simplified single-ended self-biased two stage PA is presented in Figure 3. The main difference between the latter PA and the classic architecture is the type and the biasing of the first stage. The first stage is inverter based and is biased at  $VDD/2$  via diodes  $Q_2$  and  $Q_5$ . In order to widen input  $S_{11}$  response,  $R_1$  and  $C_2$  components should be designed with caution. One of the main drawbacks of an inverter based input stage is that the input saturates at 5 dB to 10 dB lower input powers than the classic input stage. The output stage is biased for an AB class operation from an internal source.

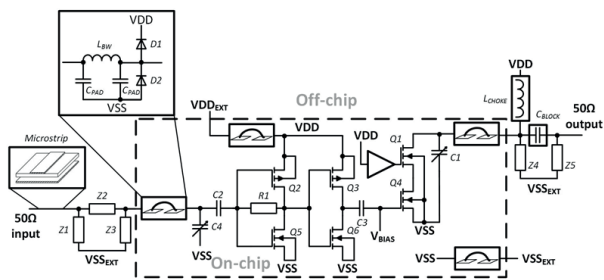


**Figure 3:** Self-biased two stage single-ended power amplifier simplified schematic

In both PA architectures, capacitors  $C_4$  and  $C_2$  act as DC blocks and also influence the overall PA stability. Digital varactors  $C_1$  and  $C_4$  are used to tune input and output impedances in order to achieve optimal power and gain matching respectively. In order to get more accurate impedance matching results, bondwire models with ESD protection diodes and microstrip feed lines (as  $S$ -parameter  $nPort$  elements) are also introduced. Both input ( $Z_1, Z_2, Z_3$ ) and output ( $Z_4, Z_5, C_{BLOCK}$  and  $L_{CHOKE}$ ) impedance matching networks are placed off-chip due to the lack of chip area. External component package parasitics were also taken into account during calculations.

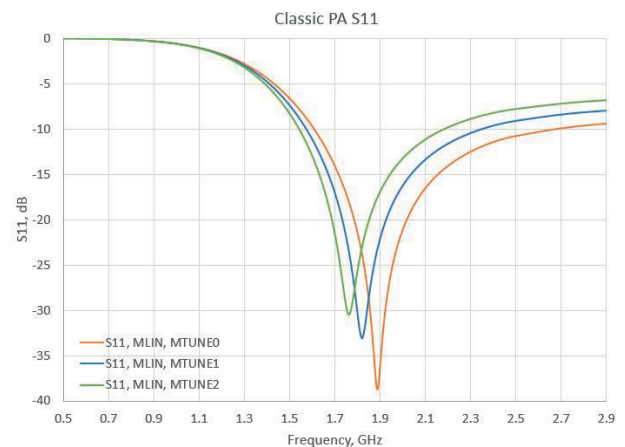
### 4 Simulation results

This chapter presents simulation results for the proposed PAs. It should be noticed, that the presented results correspond to the fully differential power amplifier configurations, whereas Figure 2 and Figure 3 present only the simplified single-ended schematics. Both PAs operate at 1.8 V supply voltage and were designed to provide a power gain of 20 dB and output power of 11 dBm to a 50 Ω load.

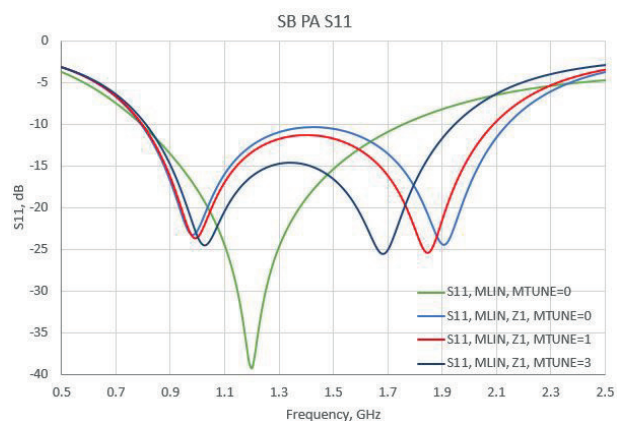
Input impedance matching results for both PA architectures are presented in Figure 4. Figure 4 (a) presents  $S_{11}$  response for the classic PA configuration with an external impedance matching network  $Z_2$  and  $Z_3$ . External matching component  $Z_2$  has been designed to be

a 1.5 pF capacitor and  $Z_3$  – a 4.2 nH shunt inductor. The matched frequency can be altered either by changing internal  $C_4$  capacitor control  $MTUNE$  value or by varying the off-chip shunt inductor  $Z_3$ . In both cases the  $S_{11}$  notch response bandwidth does not top 1.1 GHz at  $S_{11} = -10$  dB.

In comparison, Figure 4 (b) presents input impedance matching results for the self-biased PA architecture. Taking into account package parasitics and a cautious  $R_1$  (ref. Figure 3) resistor value tuning leads a naturally matched bandwidth of 1 GHz without any additional matching components (" $S_{11}$ , MLIN,  $MTUNE = 0$ " plot in Figure 4 (b)). The matching bandwidth can be further increased by introducing a series ( $Z_2$  in Figure 3) 6.2 nH inductor and altering  $MTUNE$  value.



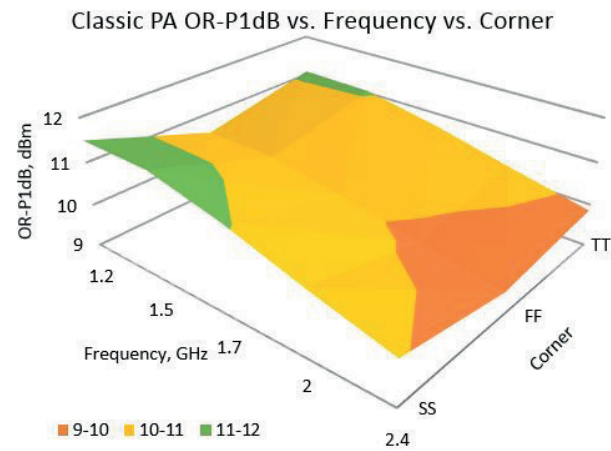
a



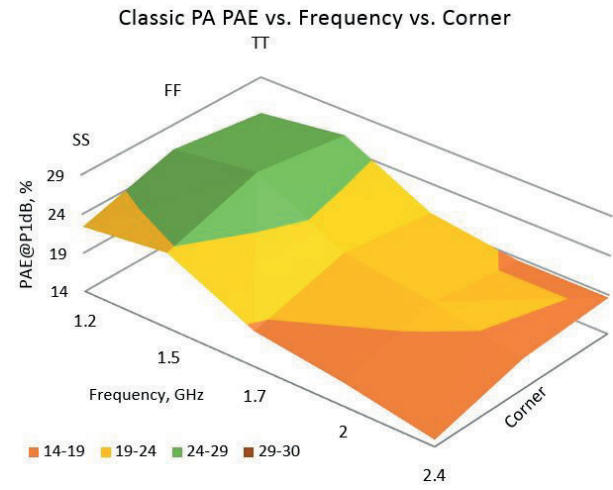
b

**Figure 4:** Classic PA (a) and self-biased PA (b)  $S_{11}$  response control

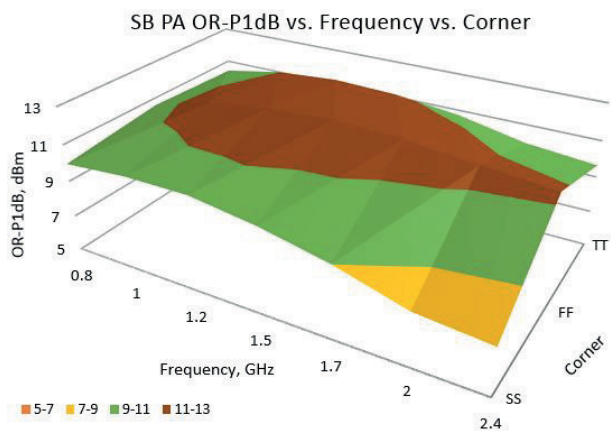
Figure 5 presents output referred 1 dB compression point (P1dB) over frequencies and corners for both PA architectures. Both power amplifiers have been designed to output an average power of 10.5 dBm.



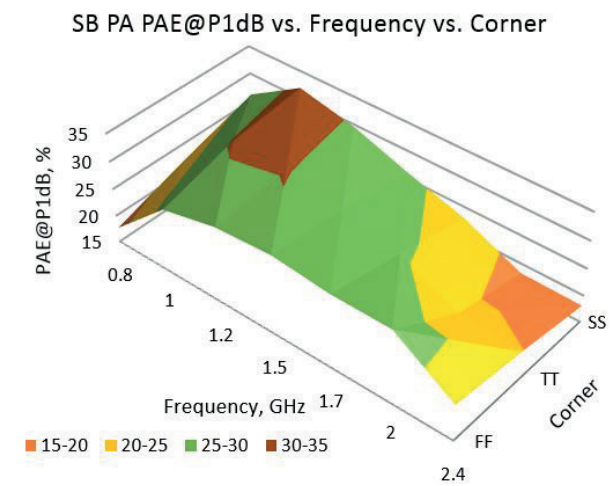
a



a



b



b

**Figure 5:** Classic PA (a) and self-biased PA (b) output referred 1 dB compression point at different frequencies and corners

Power added efficiency is presented in Figure 6. Self-biased PA average PAE is 25.3 % which is 4.2 % higher than PAE of the classic PA.

Table 2 presents the raw simulation data for surface plots in Figure 5 and Figure 6. The results presented in Table 2 depict that the self-biased PA architecture has a

**Figure 6:** Classic PA (a) and self-biased PA (b) power added efficiency at different frequencies and corners

25 % vantage in bandwidth and 1.4 % – 5.8 % efficiency at all corners and frequencies.

The layout of the designed dual differential power amplifier, implemented in IBM 7RF 0.18  $\mu\text{m}$  CMOS process,

**Table 2:** Classic and self-biased CMOS power amplifier performance comparison at different frequencies and corners

Frequency, GHz	SS	Classic PA OR-P1dB			SB PA OR-P1dB			Classic PA PAE@P1dB			SB PA PAE@P1dB		
		FF	TT	SS	FF	TT	SS	FF	TT	SS	FF	TT	SS
0.8	0.8	-	-	-	9.9	10.6	10.4	-	-	-	26.0	17.6	22.1
1.0	1.0	-	-	-	10.2	11.5	11.0	-	-	-	31.9	26.5	30.3
1.2	1.2	11.5	10.5	11.1	10.3	12.0	11.3	22.4	25.8	24.3	29.6	28.8	30.1
1.5	1.5	11.5	10.5	11.0	9.8	12.2	11.1	23.7	27.4	25.8	26.1	29.5	28.3
1.7	1.7	11.1	10.2	10.7	9.0	12.1	10.7	18.5	21.7	20.2	23.0	28.5	25.8
2.0	2.0	10.5	9.8	10.3	7.9	11.7	10.0	17.0	20.2	18.7	18.3	28.5	20.9
2.4	2.4	10.0	9.5	9.9	7.6	11.4	9.6	14.9	17.9	18.7	18.1	21.7	20.1

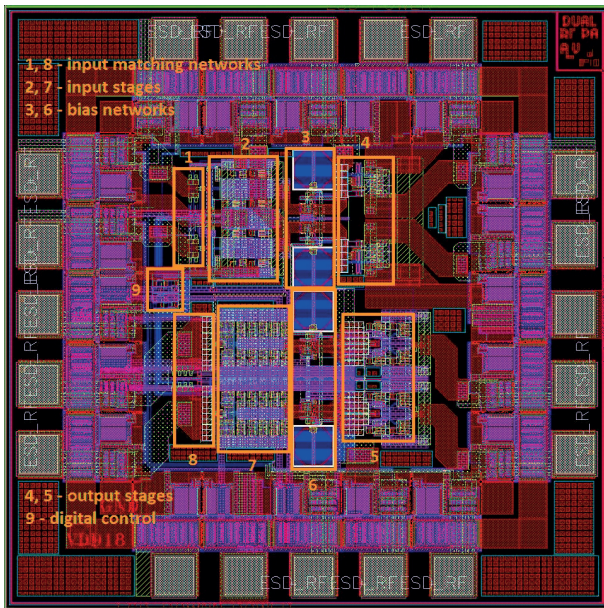


**Figure 7:** Dual differential power amplifier IC layout

IC is presented in Figure 7. PA implemented in classic architecture is presented on the top of the latter figure, and the self-biased PA – on the bottom. On-chip input matching network tuning circuits are marked 1 and 8. Active input stages are marked 2 and 7. Output stage bias networks are marked 3 and 6. Active output stages are marked 4 and 5 whereas digital control block is marked 9. The active area for both on-chip PAs is  $800 \mu\text{m}^2$ , whereas the full IC chip size is  $1.5 \text{ mm}^2$ . The dual PA ASIC has been designed to be enclosed in a 20-pin QFN package and is prepared to be send to fabrication.

## 5 Conclusion

A comparison between a classical and a self-biased PA architectures was presented in this article both suitable for a wideband Doherty configuration. Both PAs are fully differential have been implement in IBM 7RF 0.18  $\mu\text{m}$  CMOS process and are supplied from 1.8 V. Classical PA architecture has a notch type  $S_{11}$  response and a bandwidth up to 1.1 GHz (from 1.6 GHz to 2.7 GHz @  $S_{11} = -10 \text{ dB}$ ) with external matching components. Self-biased PA his matched from 800 MHz to 1.75 GHz without any additional matching components and the bandwidth can be further increased to 2.15 GHz by introducing an external matching network and by tuning the on-chip capacitance. Self-biased PA average PAE is 25.3 % which is 4.2 % higher than that of the classic PA. Both power amplifiers have an average output power of 10.5 dBm. The latter results show, that a self-biased PA architecture has more potential to be implemented in a wideband DPA configuration, compared to the

classic PA arrangement. The active area for both on-chip differential PAs is  $800 \mu\text{m}^2$ , whereas the full IC chip size is  $1.5 \text{ mm}^2$ . The dual PA ASIC has been designed to be enclosed in a 20-pin QFN package and is prepared to be send to fabrication.

## 6 References

1. Qian-Fu Cheng et al. "Investigating the global trend of RF power amplifiers with the arrival of 5G". Wireless Symposium (IWS), 2015 IEEE International. March 30 2015-April 1 2015. pp. 1-4.
2. R. Giofre, L. Piazzon, et al. "A distributed matching/combining network suitable for Doherty power amplifiers covering more than an octave frequency band". 2014 IEEE MTT-S International Microwave Symposium (IMS2014). 1-6 June 2014. pp 1-3.
3. Xian Cui, et al. "A 3.5 GHz CMOS Doherty power amplifier with integrated diode linearizer targeted for WiMax applications". MWSCAS 2007. 50th Midwest Symposium on Circuits and Systems. 2007. 5-8 Aug. 2007. pp. 465 - 468.
4. N. Ryu, J. H. Jung, and Y. Jeong, "High-efficiency CMOS power amplifier using uneven bias for wireless LAN application". ETRI J., vol. 34, no. 6, Dec. 2012. pp. 885–891.
5. C. Y. Liu. "A 2.4 GHz CMOS Doherty Power Amplifier". IEEE MTT-S International Microwave Symposium Digest, 2006. 11-16 June 2006. pp. 885 - 888.
6. J. H. Kim, et. al. "Single-Ended CMOS Doherty Power Amplifier Using Current Boosting Technique". IEEE Microwave and Wireless Components Letters (Volume: 24, Issue: 5). 06 May 2014. pp. 342 - 344.
7. N. Ryu et al. "CMOS Doherty Amplifier With Variable Balun Transformer and Adaptive Bias Control for Wireless LAN Application". IEEE Journal of Solid-State Circuits, Vol. 49, issue 6. 10 April 2014. pp. 1356 - 1365.
8. N. Wongkomet, et al. "A 1.7GHz 1.5W CMOS RF Doherty Power Amplifier for Wireless Communications". Digest of Technical Papers. IEEE International Solid-State Circuits Conference, 2006. ISSCC 2006. 6-9 Feb. 2006. pp. 1962 - 1971.
9. J. Kang, et al. "A Ultra-High PAE Doherty Amplifier Based on 0.13- $\mu\text{m}$  CMOS Process". IEEE Microwave and Wireless Components Letters (Volume: 16, Issue: 9). 28 August 2006. pp. 505-507.
10. H. H. Liao, H. Jiang, P. Shanjanani and A. Behzad. "A fully integrated 2x2 power amplifier for dual band MIMO 802.11n WLAN applications using SiGe HBT technology", IEEE RFIC Symp. Dig. 2008. pp. 515–518.

11. W. M. Gaber, et al. "A CMOS IQ Digital Doherty Transmitter Using Modulated Tuning Capacitors", 2012 Proceedings of the ESSCIRC. 17-21 Sept. 2012. pp. 341 - 344.
12. M. L. Carneiro, et al. "A 2.535 GHz fully integrated Doherty power amplifier in CMOS 65nm with constant PAE in backoff". 2013 IEEE Fourth Latin American Symposium on Circuits and Systems (LASCAS), Feb. 27 2013-March 1 2013, pp. 1-4.
13. A. Afsahi, A. Behzad, and L. E. Larson "A 65 nm CMOS 2.4 GHz 31.5 dBm power amplifier with a distributed LC power-combining network and improved linearization for WLAN applications". IEEE ISSCC Dig. Tech. Dig., 2010, pp. 452–453.
14. N. Deltimple, et al. "Integrated Doherty RF CMOS Power Amplifier design for Average Efficiency Enhancement". 2015 IEEE International Wireless Symposium (IWS). March 30 2015 - April 1 2015. pp. 1-4.
15. P. Colantonio, F. Giannini et al. "Designing a Doherty power amplifier". Melecon 2010 - 2010 15th IEEE Mediterranean Electrotechnical Conference. 26-28 April 2010. pp. 543 - 548.

Arrived: 15. 06. 2016

Accepted: 01. 07. 2016